

Research Journal of Pharmaceutical, Biological and Chemical Sciences

Utilization of Nano-Powder Barium Strontium Titanium Oxide ((BaTiO₃)(SrTiO₃)) for Improving the Properties of Acrylonitrile Butadiene Rubber.

Abd El-Aziz A. El-Wakil^{1,3}, Hesham Moustafa^{1*}, and Fahima M. Helaly².

¹Polymer Metrology & Technology Department, National Institute for Standards (NIS), Tersa Street, El Haram, P.O Box 136, Giza 12211, Giza, Egypt.

²Polymers & Pigments Department, National Research Center, Dokki, Giza, Egypt.

³Chemical Engineering Department, Faculty of Engineering, University of Hail, Hail, KSA.

ABSTRACT

This work deals to evaluate nano-powder barium strontium titanium oxide ((BaTiO₃)(SrTiO₃)), (nano-BSTO) as reinforcing filler for acrylonitrile butadiene rubber (NBR) with titanium dioxide (TO) and carbon black (CB) fillers. The bound rubber content (BRC), rheological, tensile strength property, abrasion resistance and swelling of NBR reinforced with nano-BSTO, were evaluated. The results revealed that nano-BSTO of unvulcanized NBR showed superior BRC values. The scorch time and optimum curing time of cured samples became shorter after adding the investigated fillers, whereas the torque variation increased. The mechanical properties showed higher tensile values of NBR/nano-BSTO vulcanizates containing up to 5 phr, then decreased, as compared to NBR/TO, NBR/CB or neat NBR. The effect of thermal oxidative aging at 90°C for 168 hours on tensile properties of the neat NBR and its composites was also evaluated. The scanning electron microscopy (SEM) illustrated that the utilization of nano-BSTO as filler gave superior compatible and dispersion through the investigated surface.

Keywords: Acrylonitrile butadiene rubber, bound rubber, ((BaTiO₃)(SrTiO₃)), tensile properties, abrasion resistance, swelling ratio

**Corresponding author*

INTRODUCTION

Acrylonitrile butadiene rubber (NBR) is widely used in automotive and petroleum industries due to its good processability, high abrasion resistance and high resistance to swelling in solvent and oil. It inevitably contacts oils when it is used as gaskets or seals. However, NBR exhibits poor ozone resistance and mechanical properties without vulcanization and reinforcing fillers. Therefore, elastomeric materials have to be generally reinforced with fillers such as carbon black or silica to optimize properties that meet a given service application or sets of performance parameters at high loadings [1-5]. Nowadays, nano-sized fillers such as organoclay and carbon nano-tubes have attracted the interest of researchers around the world in both industry and science due to the main advantage of these materials that, the enhanced properties can be obtained with a smaller filler content [6,7]. However, introducing better linkages between the nanoparticles and the polymer-matrix is still a challenge for specific composite fabrication [8].

Among other nano-sized fillers used with elastomers at very low concentrations compared to micro or macro sized fillers, nano- CaCO_3 [9], Cu nanoparticles [10], titanium dioxide (TiO_2) [11], and barium strontium titanium oxide ($(\text{BaTiO}_3)(\text{SrTiO}_3)$) [12] that have also become technologically important materials for improving diverse polymer properties such as mechanical, thermal, electronic and electrical properties. The mix of reinforcing nano-fillers with polymer attracts many scientists to tailor a new composite with synergic characteristic [13] or which withstands abrasion, ozone, heating aging, oil and solvents swelling with desirable mechanical properties. Hence, the new product will have excellent abrasion resistance, oil resistance, and thermal oxidative aging resistance, and mechanical strength. It could be used for the production of known rubber goods requiring such properties, e.g. automotive brake hoses, seals in motor engines, transmission belts and conveyor belts. In some cases, these fillers incorporate with polymer matrix as conductive additives to achieve their properties towards of electronic and electrical applications, especially in renewable energy sources such as solar cells [14,15].

In order to improve the dispersion of these fillers into the rubber matrix and increase the interfacial adhesion as well as the compatibility, the rubber should have functional groups in its backbone to obtain filler-rubber interaction rather than filler-filler interaction (Payne effect). This provides considerable improvement in the interfacial and mechanical properties of rubber composites. Other researchers [16,17] used hydrophilic clay with NBR or EVA and have reported that the clay needs to be modified by surfactant prior to mixing with polymer matrix. Meanwhile, others used maleic anhydride [18-21] or silane coupling agent [22,23] not only to improve the filler dispersion and compatibility but also to prevent adsorption of curatives on the silica surface. Thomas et al. [xi] reported that, the filler geometry and its particle size play an important role on the mechanical and thermal stability of the composites. In some cases, the dispersion and compatibility of rubber/filler enhanced with certain fillers such as TiO_2 , nano- CaCO_3 , Barium titanate (BaTiO_3) [24] or $(\text{BaTiO}_3)(\text{SrTiO}_3)$ without adding a coupling agent. Unfortunately, however, the nanocomposites based on $(\text{BaTiO}_3)(\text{SrTiO}_3)$ are poorly reported in the literature since there were no really needed for physico-mechanical or physico-chemical properties according to our knowledge.

The present study focused on determination of utilization nano-powder barium strontium titanium oxide ($(\text{BaTiO}_3)(\text{SrTiO}_3)$) (nano-BSTO) as filler for NBR and evaluate their properties as the bound rubber interaction, rheological and mechanical properties, abrasion resistance and swelling measurements of sulfur vulcanized NBR rubber. In comparison with some investigated conventional specific fillers such as titanium dioxide (TO), high abrasion furnace carbon black (CB), and study the effect of thermal oxidative aging on the NBR product. Also, evaluate the surface morphology of the vulcanizate containing the new investigated filler by SEM.

MATERIALS AND METHODS

Materials

Acrylonitrile butadiene rubber copolymer (NBR Kraynac, 34/50), was obtained from Polysar Co., France. Titanium dioxide (TO) with purity $\geq 99\%$ and particle size $< 4 \mu\text{m}$ supplied from Winlab, Leicestershire, LE 169 EJ, UK. Barium Strontium Titanium Oxide ($(\text{BaTiO}_3)(\text{SrTiO}_3)$) (M.Wt: 416.68), nano-BSTO used as nanopowder material with purity $> 99\%$ and particle size $< 100 \text{ nm}$ was purchased from Sigma/Aldrich Co., Germany. High abrasion furnace (HAF-LS) carbon black (CB) was obtained from Alexandria Carbon Black Co.,

Egypt. It has iodine value 82 ± 7 g/kg and adsorption behavior of dibutyl phthalate (DBP) 72 ± 7 cm³/100g. Curing ingredients, including zinc oxide, stearic acid, Tetramethylthiuram disulfide (TMTD), 2-Mercaptobenzothiazol (MBT) and sulfur, were provided by Sigma/Aldrich Co., Germany and used as received. The toluene solvent was provided from Merck. The brake oil used was supplied by Tomahawk Oil Co.,LTD, USA and the motor oil was obtained from Total (Quartz 2500 SF SAE 40), Egypt.

Preparation of NBR/ filler composites

Three different types of fillers at different concentrations were incorporated with acrylonitrile butadiene co-polymer (NBR) according to the recipe shown in Table 1. The filler contents were added in different amounts, 3, 5, and 7 phr for each type of the investigated filler. The mixing process was carried out using a conventional laboratory sized two-roll mill (152.4 x 330.2 mm) at a gear ratio 1:1.4. Each mix was pre-masticated on the mixer for 5 min before adding the filler. Afterwards, zinc oxide and stearic acid were added, followed by the addition of vulcanizing system for a total mixing time of 20 minutes to avoid premature vulcanization due to excessive heat generated during compounding. Prior to add the zinc oxide, stearic acid and curing system, 1 g of mix was taken to measure the bound rubber content. The sample codes are described in Table 1.

Table 1: The recipes of unfilled and filled NBR composites.

Ingredients, phr ^a	Neat NBR	NBR/TO			NBR/CB			NBR/nano-BSTO		
NBR	100	100	100	100	100	100	100	100	100	100
TiO ₂ (TO)	-	3	5	7	-	-	-	-	-	-
CB	-	-	-	-	3	5	7	-	-	-
Nano-BSTO	-	-	-	-	-	-	-	3	5	7
ZnO	5	5	5	5	5	5	5	5	5	5
Stearic acid	2	2	2	2	2	2	2	2	2	2
TMTD ^b	0.75	0.75	0.75	0.75	0.75	0.75	0.75	0.75	0.75	0.75
MBT ^c	0.75	0.75	0.75	0.75	0.75	0.75	0.75	0.75	0.75	0.75
Sulfur	1.5	1.5	1.5	1.5	1.5	1.5	1.5	1.5	1.5	1.5

^a part per hundred part of rubber

^bTetramethylthiuram disulfide

^c2-Mercaptobenzothiazol

Characterization and measurements

Bound rubber content

The bound rubber content (BRC) was carried out on unvulcanized rubber samples without curing agents. About 1 g of uncured sample was cut into small pieces, put into a clean glass vessel, and immersed in toluene at room temperature for seven days at normal environmental conditions. The amount of BRC, % was calculated using the following equation [25]:

$$BRC, \% = \left(\frac{W_d - W_f}{W_r} \right) * 100 \quad (1)$$

Where, W_d is the weight of sample after extraction, W_f is the weight of filler in the sample and W_r is the original weight of rubber in the sample. Three samples from each formulation were tested and the average values were recorded.

Rheological properties

Vulcanization processes were done at 150°C with frequency of 0.833 Hz, according to ASTM D2084-07, using an oscillating disc rheometer (MDR 2000), supplied by Alpha Technologies, UK. The optimum cure time, T_{c90} , of the fully specimens was determined as the time needed to reach 90% of the maximum torque in the

MDR 2000. The specimens were then vulcanized in a hydraulic hot press at 150°C for the respective cure time, T_{c90} and under a pressure of 150 kg/cm² to produce standard test specimens for tensile tests.

Mechanical testing

The tensile strength of neat NBR and its filled composites were measured according to the standard test method ASTM D 412. Sheets of dimensions 100 mm × 100 mm × 2 mm were prepared, using a hydraulic press at 150°C under a pressure of 200 kg/cm², and cure time as listed in Table 3. Type 2 dumbbell test samples were die-cut from the moulded sheets. Tensile properties were determined using a tensile testing machine (Zwick, model Z010, Germany), at a temperature of 23 ± 2°C and crosshead speed of 500 mm/min according to the standard method. To investigate the influence of thermal oxidative aging on the tensile properties (tensile strength and elongation at break), the samples were aged in an air circulating oven operated at 90 °C for different aging time as 48, 96, 144 and 168 h. The tensile properties were measured before and after the thermal aging time. At least four measurements from each sample were recorded, and the average values were reported.

Abrasion resistance measurements

Abrasion or wear resistance of the rubber vulcanizates in terms of volume loss (A) in mm³ was determined according to ASTM D 5963-97a by using Zwick abrasion tester model 6102, Germany. The cylindrical shape sample (15 mm in diameter and 12 mm in thickness) was placed at the starting position of the testing machine. The sample was then abraded across a test emery paper of grade 60 at a constant force, 10 N and constant speed, 0.32 m/s. after an abraded distance of 40 cm was reached, the sample was automatically lifted from the test emery paper. The abrasion loss or volume loss (A) in mm³ of the rubber vulcanizates was computed from the following equation:

$$A = \frac{\Delta m * S_o}{\rho * S} \quad (2)$$

Where Δm is the loss in mass in mg; ρ is the density of sample in mg/cm³; S_o is the nominal abrasive grade (200 mg); S is the abrasive grade in mg. Density of the sample (ρ) was calculated by hydrostatic method according to ASTM D 297 using Mettler Toledo's Density kit, Model: MS 2045/01, Switzerland, as follows:

$$\text{Density at } 25^\circ\text{C, } \rho, \text{mg} / \text{m}^3 = \frac{0.9971 * M}{(M - B - C)} \quad (3)$$

Where M is the mass of sample (g), B is the mass of sample and supporting wire in water (g) and C is the mass of supporting wire in water (g). Three measurements of each sample were performed and the average value was taken.

Swelling measurements

Swelling test in toluene

The degree of swelling at equilibrium, (S %) was assessed by measuring the amount of toluene absorbed. The vulcanized specimens were cut into pieces of dimensions of 15 mm x 10 mm x 2 mm and weighed, W_i , followed immersion in a toluene for 72 hours at room temperature (25 °C) [26]. During the conditioning period, the solvent was renewed after 24 hours. The swollen specimens were removed from toluene and weighed again, W_s . The specimens were then dried in an oven at 70 °C until constant weight. The degree of swelling at equilibrium (S%) for filled samples was calculated from the following equations[27]:

$$S, \% = \left[\frac{(W_s - W_f) - (W_d - W_f)}{(W_d - W_f)} \right] * 100 \quad (4)$$

Where, W_d is the weight of sample after drying and W_f is the weight of filler in the sample. Three measurements of each sample were tested and the average of the values was taken.

Swelling test in brake and motor oil

The swelling ratio (Q_{eq}) at equilibrium for rubber samples was carried out in brake oil (polar) and motor oil (non-polar) as a comparative study between two different types of oils in terms of polarity. About 0.3-0.4 g of each sample was weighed in a weighing bottle and immersed in the oil for seven days at room temperature (25°C). The swollen samples were taken out from oil and immersed again in acetone then blotted with filter paper gently, and weighed on an electronic balance. The swelling ratio of cured samples (Q_{eq} , %) was calculated from the following equation [28] :

$$Q_{eq}, \% = \frac{(W_e - W_o)}{W_o} * 100 \quad (5)$$

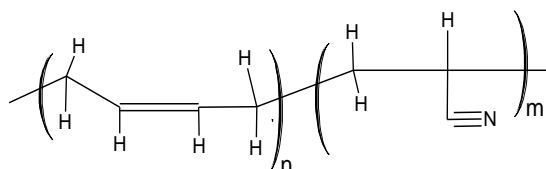
Where W_o is the initial weight of the sample and W_e is the weight at equilibrium. Experiments were run in triplicate and averaged values were reported.

Scanning electron microscope study (SEM)

The investigated filler dispersion in rubber matrix was observed using scanning electron microscopy (SEM) with a JEOL JXA-840A electron probe microanalyzer (Tokyo, Japan), with an acceleration voltage of 20 kV. The samples were previously coated with a conductive layer of gold by S150A sputter coater before analysis.

RESULTS AND DISCUSSION

The acrylonitrile butadiene rubber was chosen as a type of synthetic rubber of high polarity because of the presence of nitrile group along the carbon chains that raise the glass transition temperature (T_g) which was found approximately -45°C. The chemical structure of NBR is:



The investigated formulations of NBR mixes are illustrated in Table 1.

Bound rubber measurements through rubber-filler interaction

Bound rubber test was carried out on the unvulcanized filled rubber using toluene as solvent at room temperature. The bound rubber content is a function of the interaction between filler and rubber [29]. Table 2 shows a comparison of BRC of NBR in the range from micro- to nano-fillers; it can be observed that, the amounts of BRCs determined for samples based on nano-filler (e.g. nano-BSTO) are higher than those measured for samples based on investigated conventional fillers (e.g. TO and CB). This may be due to not only the particle size of nano-fillers but also the better rubber-nano-filler interaction as compared to rubber/micro-filler interaction. The obtained results confirmed with that of Choi et al. [30] who reported that the level of bound rubber formation is basically dependent on the surface chemical active groups into the filler and polymer molecular weight, as well as the filler-matrix interaction, where the stronger the filler-rubber interaction resulted in the more bound rubber is formed [xxix]. It is also noticed that BRC values of NBR/TO sample is 60.86% at 3 phr filler content and 70.24 % for NBR/CB at 5 phr filler content. This implies that, the filler dispersion at low concentration (i.e., lower agglomeration structure in the rubber matrix) play a significant role in the bound rubber formed.

Table 2: The bound rubber content of compounded rubber mixes.

Specimens	Filler loading, phr	Bound rubber content (BRC), %
NBR/TO	3	60.86 ± 0.65
	5	19.50 ± 0.72
	7	35.76 ± 0.57
NBR/CB	3	41.90 ± 0.43
	5	70.24 ± 0.35
	7	49.84 ± 0.55
NBR/nano-BSTO	3	88.06 ± 0.62
	5	84.22 ± 0.70
	7	83.41 ± 0.45

Rheological properties

Table 3 shows the rheological characteristics of compounded rubber mixes, as scorch time (T_{s2}), optimum curing time (T_{c90}) and torque variation ($M_{max}-M_{min}$) of filled NBR composites from micro- to nano-fillers, and compares them to the gum NBR composite. The T_{s2} and T_{c90} of all filled NBR composites were decreased while the torque variation increased in the presence of investigated fillers as compared to neat NBR. The torque variation apparently is an indication to the cross-link density of the rubber vulcanizate [31]. As can be seen, its values increased in the presence of filler as in case of TO, CB and nano-BSTO filler types. The obtained data, also showed that, the torque variation in case of filled NBR composites based on TO and nano-BSTO fillers decrease with increasing the filler loading. This decrease may be caused by the formation of filler-filler interactions (i.e. the inter-aggregate distances become smaller with rising filler content), which are formed with filler loading, and therefore the probability for the formation of a filler network increases [32].

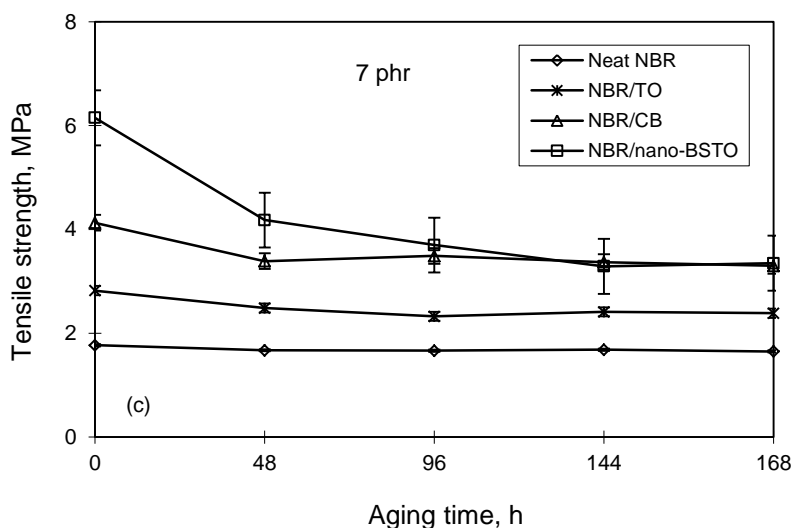
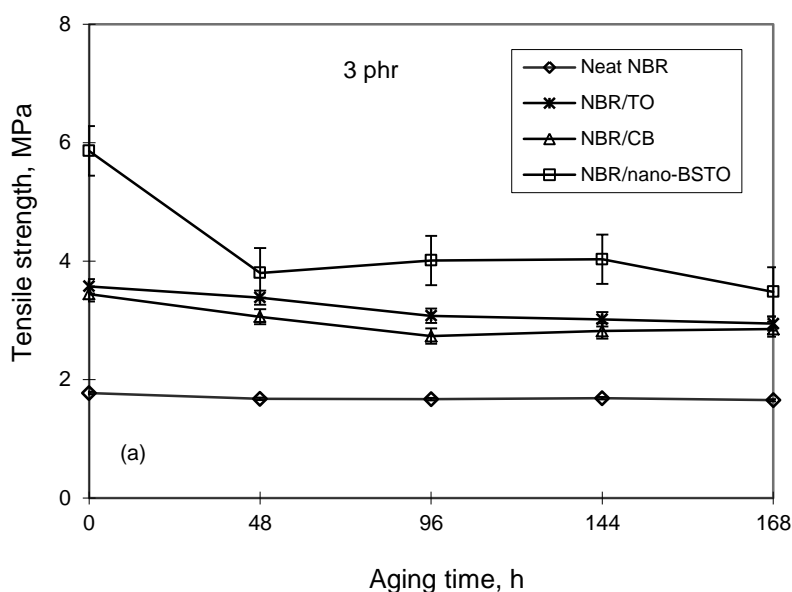
Table 3: Rheological characteristics of unfilled and filled NBR composites.

Specimens	Filler loading, phr	Rheological characteristics		
		T_{s2} , min ^a	T_{c90} , min ^b	$(M_{max}-M_{min})^c$ (dNm)
Neat NBR	-	2.21	5.50	8.34
	3	1.23	3.50	13.90
NBR/TO	5	1.45	3.50	12.40
	7	1.60	4.00	11.90
NBR/CB	3	1.82	4.50	10.00
	5	1.34	4.00	12.50
	7	1.55	3.60	12.32
NBR/nano-BSTO	3	1.56	4.47	11.50
	5	1.50	4.30	10.40
	7	1.35	4.94	10.15

Evaluation of mechanical properties

The mechanical properties of unfilled NBR and its filled composites were tested before and after thermal oxidative aging at 90°C for 168 h. Fig. 1(a,b and c) shows the mechanical properties of NBR containing different concentrations of fillers before and after aging. The concentrations of fillers are introduced in the NBR matrix ranged from 3 to 5 phr, the tensile properties improved as compared to gum rubber. This is due to the reinforcement effect which is directly related to the specific nature of the filler interface that causes interactions between rubber and fillers [33]. Fig. 1a displays the tensile strength of neat NBR and its filled composites based on 3 phr from TO, CB and nano-BSTO as a function of aging time. It was found that as the aging time increase, the tensile strength decrease to a certain aging time (48 h) in case of NBR/nano-BSTO nanocomposite, and to 96 h in case of NBR/TO and NBR/CB composites. Further increase in aging time, the former one re-increased until 144 h, then decreased but its tensile values were still much better in comparison with the two latter and neat NBR, which were remained the same with increasing the aging time. The figure also shows that the tensile values of NBR/TO composite contained 3 phr filler content are higher as compared to NBR/CB composite. This may be due to the specific interactions between rubber macromolecules and the

active filler sites. These interactions are described by the compatibility and the good dispersion of the filler with the rubber matrix. With further increase in the loading of the filler, the tensile properties were firstly increased, especially in case of 5 phr nano-BSTO, and then started obviously to decrease at 48h with increase the aging time in case of NBR/nano-BSTO nanocomposites, including NBR/TO, NBR/CB or neat rubber, as shown in Fig. 1(b,c). Moreover, NBR/CB composite exhibited higher tensile properties at 5 phr and 7 phr filler loading as respect to NBR/TO composite. Based on the tensile data, it can say that, three parts per hundred rubbers seems to be the optimum filler loading for TO, up 5 phr for CB and in between 3 and 5 phr for nano-BSTO. These data were confirmed with the results obtained by other researchers [34]. They reported that the mechanical properties of incorporated nano-TiO₂ in NR matrix enhanced at lower filler loading due to a better dispersion and good homogeneity of nano-TiO₂ in the matrix. Also, Thomas et al. [35] studied the mechanical properties of TiO₂ filled polystyrene (PS) and found that the tensile strength reached a maximum value at 5 wt.% addition of TiO₂. Balachandran and Bhagawan [36] have reported that the tensile strength increased rapidly with increasing nanoclay content in the range from 2 to 5 phr and decreased thereafter because of the formation of aggregates and the poor dispersion at higher filler content.



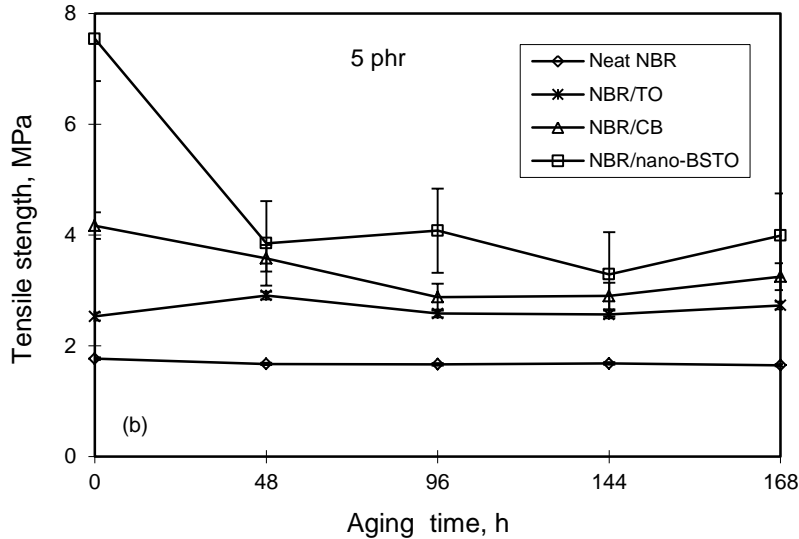
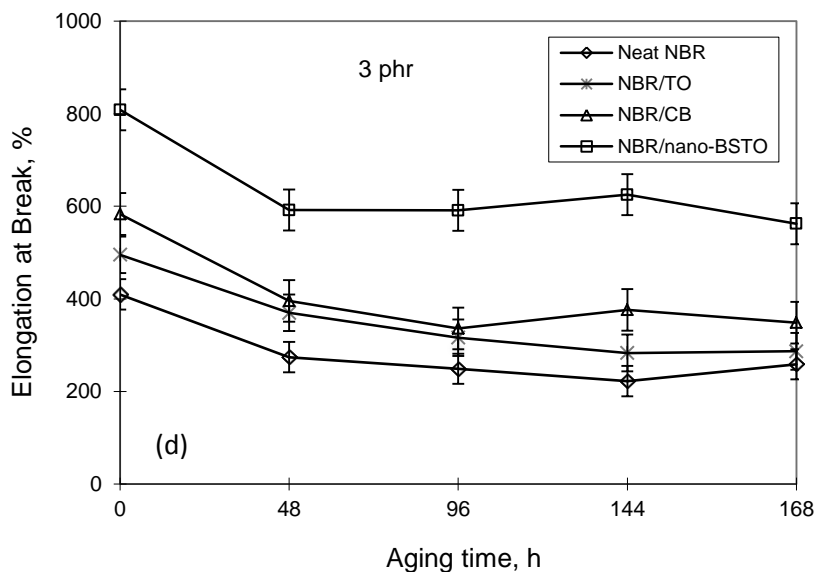


Fig. 1: Variation of tensile strength of unfilled and filled NBR composites according to aging time (a) 3 phr, (b) 5 phr and (c) 7 phr filler loading.

Similarly, Fig. 2 (d,e and f) shows the elongation at break of neat NBR and filled composites before and after thermal oxidative aging at 90 °C for 168 h. Based on the obtained results, it is worthy to note that, nano-BSTO filler improves the elongation at break of the NBR nanocomposites in comparison with NBR/TO, NBR/CB and neat rubber. This improvement may due to the lower nanoparticle size and the good dispersion of nano-BSTO in the NBR matrix that help to increase the elasticity of NBR chains. increasing the time of thermal oxidative aging, the elongation at break values were decreased (after 48 h) , and then these values seems to be remained with a good thermal aging until 168 h in all composites, including the neat rubber, as shown in Fig. 2 (d,e and f). As expected from above, the mechanical properties (tensile strength and elongation at break) of NBR/nano-BSTO nanocomposites are better than that of the NBR/TO and NBR/CB composites containing the same investigated filler contents. This enhancement can be linked to the better dispersion of nanoparticles (nano-BSTO) besides interaction between BSTO nanoparticles and NBR matrix, the efficient reinforcement originated from the good dispersion and homogeneous distribution of nano-BSTO in the rubber matrix leading to higher reinforcement as can be confirmed with the determined value of bound rubber, as shown in Table 2.



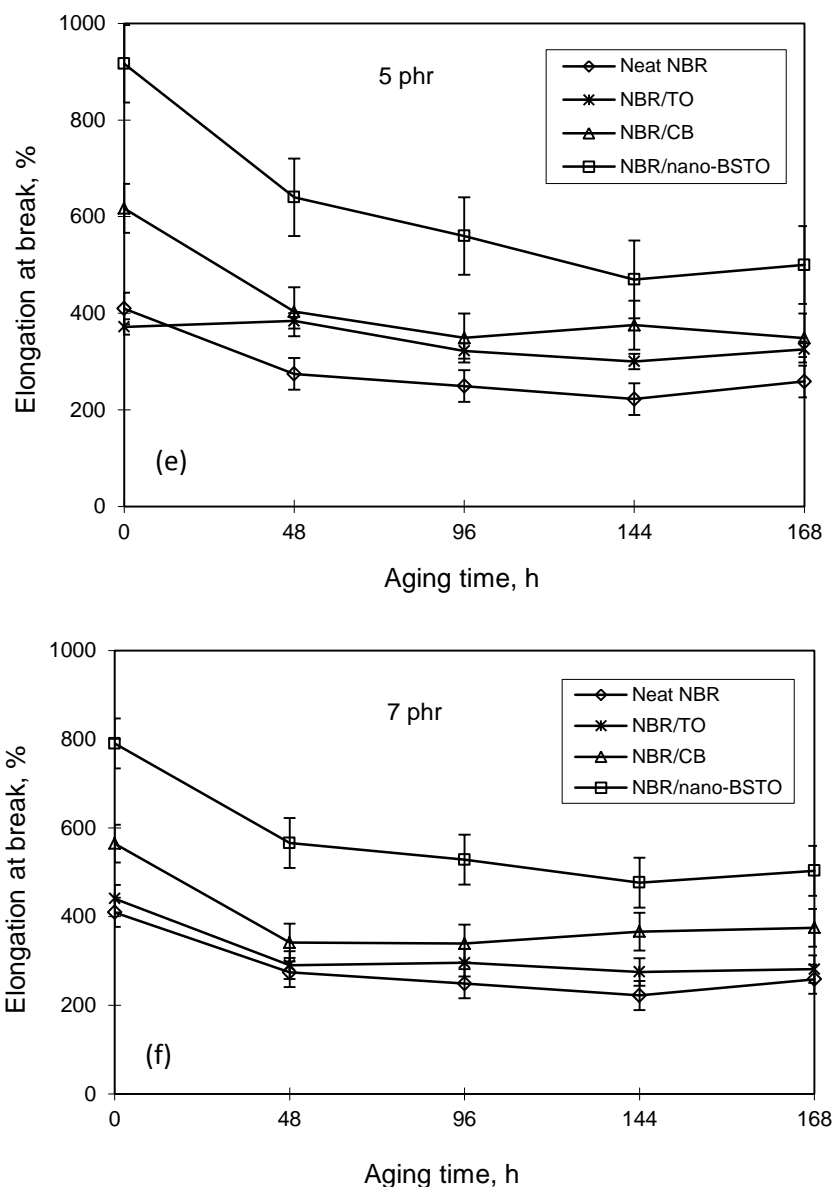


Fig. 2: Variation of elongation at break of unfilled NBR and its filled composites according to aging time (d) 3 phr, (e) 5 phr and (f) 7 phr filler loading.

Abrasion resistance

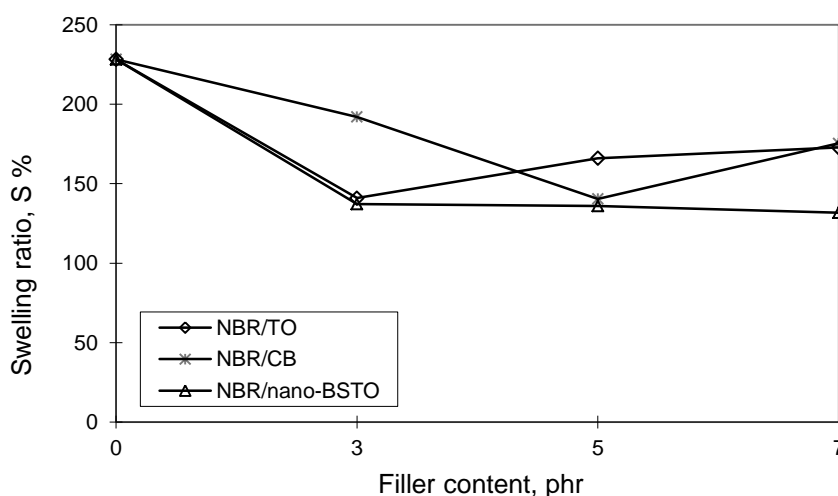
Abrasion resistance of filled rubber vulcanizates in comparison with neat NBR was determined in terms of volume loss in mm^3 . Table 4 shows the abrasion resistance for rubber vulcanizates contained different types and loadings of the investigated fillers. The presence of TO, CB and nano-BSTO in small amounts generally improved the abrasion resistance of NBR composites as compared to neat rubber. In the case of NBR/nano-BSTO composites, a remarkable reduction of volume loss (i.e., higher abrasion resistance) was obtained, especially at 3 and 5 phr contents. This could be attributed to better dispersion and distribution of BSTO nanoparticles in the rubber matrix comparing to those of other composites or unfilled NBR. In the same sense, Tabsan et al. [37] observed that the lowest volume loss of natural rubber filled by organoclay (OMMT) was obtained at 3 phr filler content. The obtained results also showed that the volume loss increased with increasing the TO contents, as shown in Table 4. The reason may result from the aggregation of TO in the NBR matrix at higher loadings. Otherwise, the rubber vulcanizates based on CB have improved the abrasion resistance with increasing CB loadings. This was confirmed to the results obtained by other researchers [38,39]. They reported that the addition of reinforcing fillers at higher loading (i.e., carbon black) in the matrix improve abrasion resistance by suppressing tearing of rubber matrix.

Table 4: Abrasion resistance for neat NBR and its filled composites.

Specimens	Filler loading, phr	Abrasion or volume loss, mm ³
Neat NBR	-	231 ± 0.90
	3	103 ± 0.45
	5	113 ± 0.57
NBR/TO	7	124 ± 0.66
	3	108 ± 0.52
	5	102 ± 0.36
NBR/CB	7	104 ± 0.75
	3	95 ± 0.33
	5	99 ± 0.42
NBR/nano-BSTO	5	99 ± 0.42
	7	107 ± 0.48

Swelling measurements

The swelling ratio (S %) of the vulcanizates as a function of filler content in toluene solvent and two different types of oil are shown in Figs. (3-5). Fig. 3 showed the degree of swelling in solvent was considerably decreased with increasing the filler content, for the rubber samples containing 3 phr of BSTO and TO compared to 5 phr for CB. The key factors for the improvement in the degree of swelling may be attributed to the better filler dispersion at low concentration and the nature of filler structure. These parameters can affect solvent penetration into the gaps between rubber macromolecules and thus decrease the swelling percentage [40]. The figure also indicated that after 3 phr and 5 phr for TO and CB, the swelling ratio started to increase, whereas there was no changes occurred at this ratio with increasing the nano-BSTO filler content.


Fig. 3. Swelling ratio as a function of filler content for unfilled and filled NBR composites in toluene.

Figs 4, 5 represent the swelling ratio of the unfilled NBR and its filled composites in motor and brake oil. Fig. 4 shows the variation of swelling ratio (Q_{eq} %) according to filler content in brake oil as polar oil at different filler types, TO, CB and nano-BSTO reinforced NBR vulcanizates. It can be seen that the percentage of oil uptake was drastically decreased with increasing the investigated filler content up to 5 phr as in case of NBR/nano-BSTO matrix compared to NBR/TO and NBR/CB matrices. These results may be due to is confirmed that to the nano-size particles of nano-BSTO which is a significant factors affecting the swelling ratio. The figure also showed that the percentage of oil uptake was slightly increased after 5 phr for all investigated fillers in the vulcanizates, as a result of the filler aggregation in the matrix. Fig. 5 shows the similar patterns of swelling percentage in motor oil as non-polar oil. From the two figures, it is observed that the polarity of oil plays an important factor affecting the swelling degrees, especially when the rubber has an active group in its backbone, since the non-polar oil shows the lower swelling degrees than the polar oil.

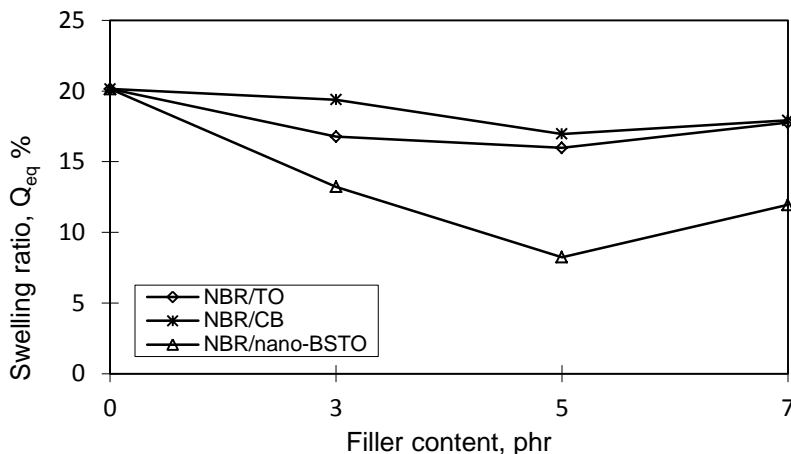


Fig. 4: Swelling ratio for unfilled and filled NBR composites in brake oil (polar).

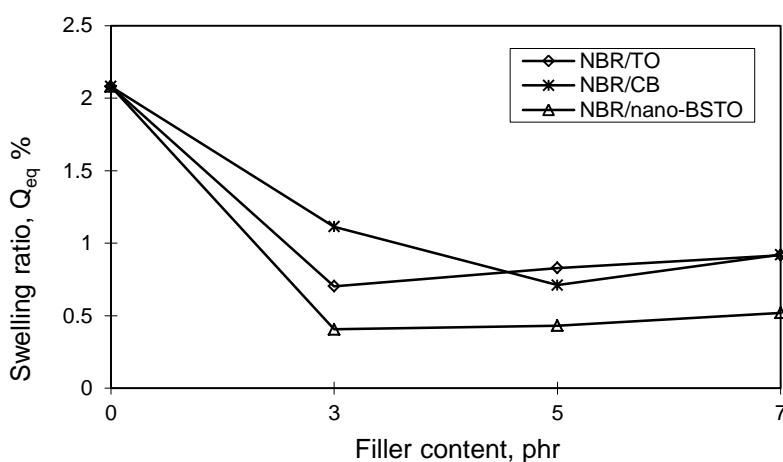


Fig. 5: Swelling ratio as for unfilled and filled NBR composites in motor oil (non-polar).

Scanning electron microscopy (SEM)

SEM is an interesting technique that offers simplest investigative procedure to reveal surface features of the investigated composites. Fig. 6(a, b and c) shows the surface texture of the neat NBR, NBR/TO and NBR/nano-BSTO. It was shown that, compatible smooth surface for the neat rubber, Fig. 6(a). Also, it is illustrated regular distribution and dispersion as well as good compatibility and homogeneity of TO and nano-BSTO on the NBR matrix, Fig. 6(b and c).

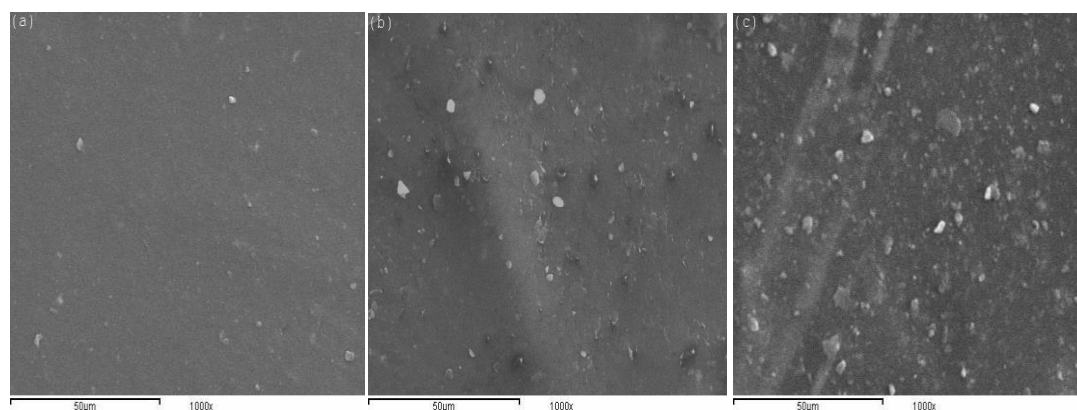


Fig. 6: SEM images for (a) neat NBR, (b) NBR/TO (3 phr), and (c) NBR/nano-BSTO (5 phr).

CONCLUSION

The amounts of BRCs determined for samples based on nano-filler (e.g. nano-BSTO) are higher than those measured for samples based on micro-fillers (e.g. TO and CB). The rheological characteristics showed that the T_{s2} and T_{c90} of all investigated filled NBR composites were decreased while the torque variation increased according to the type of the fillers under investigation. The mechanical properties (i.e., tensile strength and elongation at break) of NBR/nano-BSTO nanocomposites at 3 and 5 phr of the investigated filler are better than that of NBR/TO, NBR/CB composites or neat rubber, it was also found that increasing the time of thermal oxidative aging, these properties started slightly to decrease after 48h. The presence of the investigated fillers (i.e., TO, CB and nano-BSTO) in small amounts enhanced the abrasion resistance of rubber composites. The degree of swelling values in toluene, brake oil, and motor oil of NBR /nano-BSTO nanocomposite were lower than NBR/TO and NBR/CB composites and their values depended upon the polarity of oil. A good dispersion and interaction between nano-filler and rubber matrix were achieved and confirmed by SEM.

REFERENCES

- [1] Choi S-S. *J ApplPolymSci*2001; 79(6): 1127–33.
- [2] Ten Brinke JW, Van Swaaij PJ, Reuvekamp LAEM. *Kaut Gummi Kunst*2002; 55: 244-254.
- [3] Boretti LG, Gradwell MHS, McGill WJ. *Plast Rubber Compos* 2000; 29: 144-148.
- [4] Fan RL, Zhang Y, Li F, Zhang YX, Sun K, Fan YZ. *Polym Test*2001; 20(8): 925-935.
- [5] Choi S-S. *Polym Adv Technol* 2002;13(6): 466-474.
- [6] Wu YP, Jia QX, Yu DS, Zhang LQ. *J ApplPolymSci*2003; 89: 3855–8.
- [7] Zhang WA, Chen DZ, Xu HY, Shen XF, Fang YE. *EurPolym J* 2003; 39(12): 2323–28.
- [8] Zhijun S, Zhigang L, Donghua W, Pan Z, Wanyou L, Yingjie Q, Ruiliang L, Shi Z. *J Wuhan UnivTechnol* 2013; 28: 658-63.
- [9] Fernandez SS, Kunchandy S. *Asian J Chem* 2013; 25(15): 8638-42.
- [10] Zhou X, Zhao G, Niu H, Liu Y. *J Mater Sci.-Mater El* 2011 ; 22 : 1737–43.
- [11] Thomas PC, Thomas PS, George G, Thomas S, Kuruvilla J. *J Polym Res* 2011;18: 2367–78.
- [12] Kim SW, Choi HI, Lee MH, Park JS, Kimb DJ, Do D, Kim MH, Song TK, Kim WJ. *Ceram Int* 2013; 39: S487–S490.
- [13] Patel MV, Dolia MB, Patel JN, Patel RJ. *React FunctPolym* 2005;65(3):195–204.
- [14] Xiong J, Yang B, Zhou C, Yang J, Duan H, Huang W, Zhang X, Xia X, Zhang L, Huang H, Gao Y. *Org Electron* 2014;15: 835–43.
- [15] Monica L-C, Amine C, Jeremy F, Irene G-V, Youhai Y. *Sol Energ Mat Sol C* 2011 ; 95 :1362–74.
- [16] Ahmadi SJ, G'Sell C, Huang Y, Ren N, Mohaddespour A, Hiver J-M. *Compos Sci Technol* 2009;69:2566-72.
- [17] Beltran M I, Benavente V, Marchante V, Marcilla A. *Appl Clay Sci* 2013; 83-84:153-161.
- [18] Moustafa H, Darwish NA. *Int J AdhesAdhes* 2015;61:15–22.
- [19] Zheng X, Jiang DD, Wilkie CA. *PolymDegrad Stab* 2006; 91: 108-13.
- [20] Moustafa H, Darwish N A, Helaly FM. *J Int Environ Appl Sci* 2014 ;9(4):534-42.
- [21] Murilloa EA, López BL. *Prog Org Coat*2015;78: 96–102.
- [22] Goerl U, Hunsche A, Mueller A, Koban HG. *Rubber ChemTechnol* 1997; 70(4): 608-23.
- [23] Ten Brinke JW, Van Swaaij PJ, Reuvekamp LAEM, Noordermeer JWM. *Kaut Gummi Kunstst* 2002;55: 244-54.
- [24] Goyal RK, Katkade SS, Mule DM. *Composites: Part B*: 2013;44: 128–132.
- [25] Wolff S, Wang M-J, Tan E-H, *RubberChemTechnol* 1993;66:163-177.
- [26] Yan H, Sun K, Zhang Y, Zhang Y. *Polym Test* 2005;24: 32–38.
- [27] Kang D, Kim D, Yoon S-H, Kim D, Barry C, Mead J. *J Mater Eng* 2007;292: 329–338.
- [28] Mostafa A, Abouel-Kasem A, Bayoumi MR, El-Sebaie MG. *Mater Design* 2009;30:1561–1568.
- [29] Aranguren MI, Mora E, Macosko CW. *J Colloid InterfSci* 1997;195: 329-37.
- [30] Choi S-S. *Korea Polym J* 2001;9(1): 45-50.
- [31] Jovanovic V, Samarzija-Jovanovic S, Budinski-Simendic J, Markovic G, Marinovic-Cincovic M. *Composites: Part B*: 2013;45: 333–340.
- [32] Fröhlich J, Niedermeier W, Luginsland H-D. *Composites: Part A*: 2005;36: 449–460.

-
- [33] Arrighi V, Gagliardi S, Higgins JS, Triolo A, Zanotti J-M. Quasielastic neutron scattering as a probe of molecular motion in polymer-filler systems. E-MRS spring meeting, N-15, Strasbourg, France, 2002.
- [34] Seentrakoon B, Banja J, Warinthorn C. *PolymDegrd Stab* 2013;98: 566-78.
- [35] Thomas SP, Joseph K, Thomas S. *Mater Lett* 2004;58: 281-89.
- [36] Balachandran M, Bhagawan SS. *J Polym Res* 2012;19: 9809.
- [37] Tabsan N, Wirasate S, Suchiva K. *Wear* 2010;269: 394-404.
- [38] Xu D, Krager-kocsis J, Schlarb AK. *J Mater Sci* 2008;43: 4330-39.
- [39] Gent AN, Pulford CTR. *J ApplPolymSci* 1983;28(3): 943-60.
- [40] Abdul Kader M, Bhowmick AK. *PolymDegrd Stab* 2003;79: 283-95.